A soft-exosuit enables multi-scale analysis of wearable robotics in a bipedal animal model

S. M. Cox, Jonas Rubenson[§], and Gregory S. Sawicki[§]

***Abstract*—Wearable robotics offers a unique opportunity to explore the fundamental science of integrated systems with both engineered and biological parts. But, lacking a mechanistic understanding of the biological response to assistive technologies, the state of the art in design development is presently a sophisticated form of automated trial and error. Progress is hampered by the restrictions of human experimentation that make it difficult to assess the direct impact of wearable robots on underlying muscles, tendons and bones. The next stage of development in wearable robotics requires expanding studies 'under the skin' and 'out into the world'. Developing animal models to explore locomotion with wearable robotics could offer the opportunity to answer questions up and down the broader spatiotemporal scale that are not currently possible in humans. To fill this gap, we have built the first ever wearable robotic device for a freely-locomoting, non-human, bipedal animal (*Numida melaegris* = Guinea fowl), a species whose gait closely mirror human locomotion mechanics. We found that a passive soft-exosuit design that parallels current human passive-elastic ankle exoskeletons in function was both well tolerated and provided consistent torques. Preliminary data showed birds systematically change their kinematics in response to changes to exo-suit spring stiffness, adjusting the timing but not magnitude of the assistive torques. This animal model for wearable robotics allows us to address questions from short-term adaptations in musculoskeletal dynamics and sensorimotor signaling within a single step to broader behavioral and physical changes that come with long term use from whole-body down to individual muscles and nerves.**

I. Introduction

Wearable robotics, a rapidly expanding field at the human-machine interface[1]–[3], offers a unique opportunity to explore the fundamental science of integrated systems with both engineered and biological parts. But, lacking a mechanistic understanding of the biological response to wearable robotics, the state of the art in design development is presently a sophisticated form of automated trial and error[4]. Progress is hampered by the restrictions of human experimentation that make it difficult to assess the direct impact of wearable robots on underlying muscles, tendons and bones, with most analyses focused primarily at the whole body and lower-limb-level of human subjects tethered to large laboratory-based robotic testbeds[2], [5]–[7]. The next stage of development in wearable robotics requires expanding studies 'under the skin' and 'out into the world'. Targeted, *in vivo* measurements are necessary to provide a basic science understanding of how a user's physiological systems adapt to assistive technologies in the short and long term. The most viable approach to achieving this is to perform these studies on an animal surrogate[8]–[10]. However, unlike most major breakthrough technologies in the biomedical sciences, wearable robotics lacks an animal model with which to conduct invasive or long-term experiments.

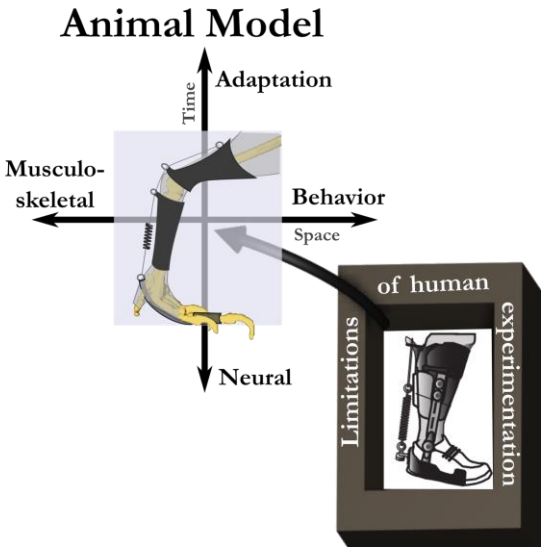

Figure 1: An animal model for wearable robotics overcomes the limitations of human experimentation, expanding spatial and temporal scales of research.

To fill this gap, we present here the first ever wearable robotic device for a locomoting [11] animal model, RoboBird. Our design (hereafter: 'exo-tendon') parallels current human passive, elastic ankle exoskeletons in function[1], [11], [12]. An untethered exo-tendon for a bipedal animal (*Numida melaegris*) whose locomotor mechanics closely mirrors that of humans[13], [14] and has been a model organisms for in-vivo locomotor studies[15]–[18] enables the study of the influence of wearable robotics on structure-function relationships up and down the temporal and spatial ladder from short-term adaptations in musculoskeletal dynamics and sensorimotor signaling within a step to broader behavioral and physical changes that come with long term use (Fig 1).

II. Methods

A. Design

The goal of this work was to build a passive-elastic exo-tendon that would be tolerated by guinea fowl during walking and running and generative assistive torques at the ankle and tarsometaphalangeal (Tmp) joints. The fundamental challenge was to design an exo-tendon with the structural integrity to provide adjustable but consistent parallel elasticity (with

*Research supported by a Huck Life Sciences and the College of Health and Human Development seed-grant to J.R., Penn State University.

S. M. Cox and J. Rubenson are with the Biomechanics Laboratory/ Muscle Function and Locomotion Laboratory, Department of Kinesiology, Pennsylvania State University, University Park, PA 16802 USA (e-mail: smc288@ psu.edu, e-mail: jxr75@psu.edu).

G. S. Sawicki is with the School of Mechanical Engineering & School of Biological Sciences, Georgia Institute of Technology, Atlanta, GA 30332 USA (e-mail: gregory.sawicki@me.gatech.edu).

§ J.R. and G.S.S contributed equally to this work as co-senior authors

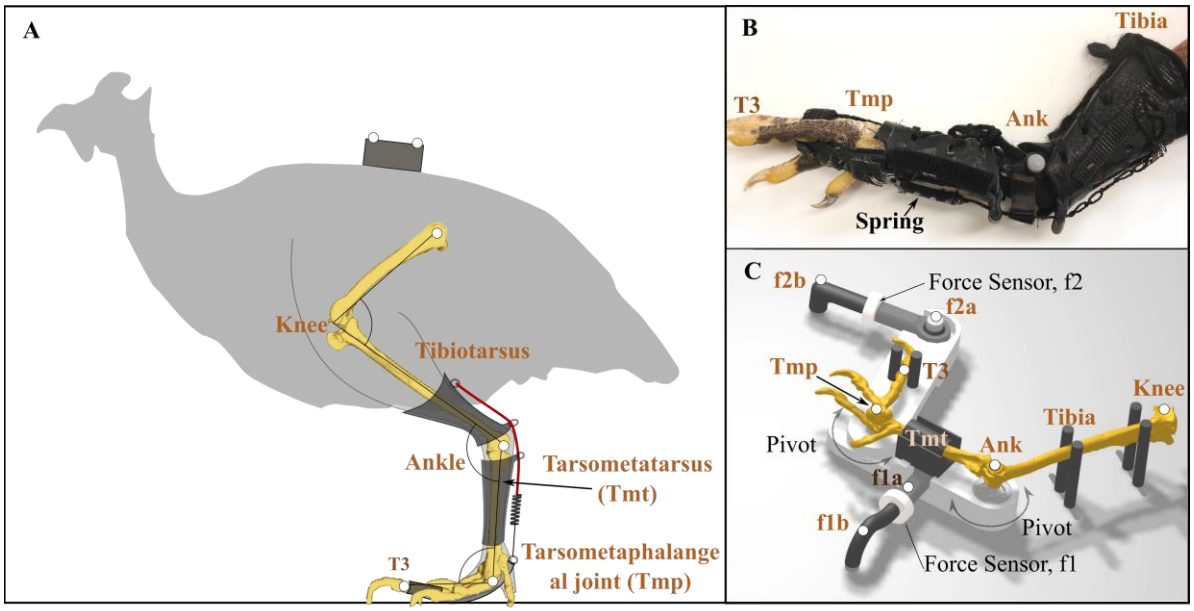

Figure 2 A) Spring path of the exo-tendon (red) spans the ankle and TMT joints of the guinea fowl, mirroring the path of several digital flexor muscles. Marker positions used for motion capture shown as white circles. B) Exo-tendon structure consists of laced leather cuffs encircling the toe, the TMT and the tibia connected by a spandex layer. The spring attaches at the proximal end of the tibia cuff, travels through guides along the posterior of the tibia and Tmt cuffs and connects to a tab extending off the toe cuff (T3). C) Tabletop jig for quantification limits joint motion to planar kinematics constrained by pin joints. The forces necessary to hold the limb at a series of configurations are compiled to generate a moment-angle surface map.

biological tendon springs) while simultaneously minimizing discomfort and mass.

We found that a soft-exosuit design that distributed interaction forces over a large surface area and was coated with a soft polymer to improve adhesion was both well tolerated and provided consistent torques (Fig 2A&B). A soft-exo laced leather structure distributes forces, minimizes discomfort and provides attachment points for the interchangeable, variable length springs. The spring path spans the ankle and MTP joints (Fig 2B), mirroring the path of several digital flexor muscle-tendon units and supplementing both joint torque and elastic energy storage during stance phase. The exo-tendon consists of three reinforced leather cuffs encircling the tibiotarsus (tibia) above the ankle, the tarsometatarsus (Tmt) and the third phalanges connected by a spandex layer. The tibia and Tmt cuffs were held snug with laces that distribute the contact forces throughout the structure. Interchangeable springs are attached to split rings threaded through reinforced portions of the proximal femur cuff and a reinforced tab extending from the toe cuff to just past the TMP joint (Fig 2B). The spring path was constrained by channels along the posterior of the femur and Tmt cuffs. Four 3 cm long springs (0.3, 0.6 1.0 and 2.3 NM) were connected to a cord with a crimp closure resulting in a slack length that that could be adjusted (Figure 2B). The exo-tendon weighs 0.028 kg/limb with springs and measures 0.17 m long. Since the spring path spans both the ankle and Tmp joints, the moment contributed by the exo-tendon at each joint is a function of both ankle and Tmp angles. Thus, flexion of the phalanges act as a natural clutch, disengaging the device during swing phase [14]

B. Animals

Eight helmeted guinea fowl (Numida meleagris) were obtained as 1 day-old keets (GuineaFarm) and housed in pairs in 1 m^2 pens, with food and water provided ad libitum on a 12h:12h light:dark cycle until skeletally mature. Animals were trained 3-4 times per week to run on a motorized treadmill. The exo-tendon design results reported here are from one animal (1.79 kg). The experimental protocol was approved by the Pennsylvania State Institutional Animal Care and Use Committee (IACUC Ref #7295). All values are listed as means$\pm$ one standard deviation.

C. Quantification

Quantification of the moment contributed by the exo-tendon at the ankle and Tmp joints were calculated in a two stage process. First, the contribution of the exo-tendon to each joint moment was determined for each biologically relevant joint angle combination. This was then combined with kinematic data collected from the bird walking in the exo-tendon to quantify the exo-tendon's contribution across the stride cycle.

1) Benchtop Moment Jig

Since the exo-tendon spring path is bi-articular, the moment contributed by the exo-tendon at each joint is a function of both the ankle and Tmp angles. Mapping of the surface of this moment-to-angle space was accomplished with the aid of a force-instrumented tabletop jig (Fig 2C). The jig constrains the motion of the ankle and Tmp joints to one plane by clamping the femur, tarsometatarsus and phalanges to three rigid arms joined by ball bearing guided pin joints (Fig 2C). The phalangeal segment connects to the Tmt segment within a slot that allowed adjustment of the distance between

the Tmp and ankle joints to account for variation in Tmt bone lengths between individuals. The phalangeal and Tmt segments were spaced up from the surface to reduce friction and the plane of motion was horizontal to minimize the influence of gravity. Adjustable pins clamped the phalanges and femur while the Tmt was restrained with a coil of Velcro. Two 1D force sensors (Omega LC201-25) connect approximately perpendicular from each segment with ball joint rod ends, allowing measurement of the force required to hold the limb at a particular configuration. Exact line of action was determined with motion analysis (described below).

2) Jig Data Collection

Quantification of exo-tendon joint moment contributions were conducted under anesthesia (isoflurane 2% induction/1.5% maintenance) by laying the bird it on its side and clamping left limb in the benchtop jig. We combined force data (300 Hz) and 3D joint kinematics using a 4-camera motion-capture system (Motion Analysis Cortex version 6.0, 300 frames/sec). Two in-line retro-reflective markers were placed along each force sensor to define the line of action of the force sensor. Markers were also placed at joint centers of the hip, ankle, Tmp and the tip of the third phalanges to enable joint angle calculations following Rubenson and Marsh (2009) [9] (Fig 2C). The limb was sequentially positioned in a series of static joint configurations (~3 sec/position) to fully map the moment space (mean 8.54e3±7.3e3 configurations/trial) while collecting simultaneous force and kinematic data. Static positions were used because they minimized moments generated due to limb acceleration. This procedure was performed in 14 settings per bird: 1) without the exo-tendon; 2) with the exo-tendon with no spring, and; 3-14) for each of the four spring at three slack lengths.

3) Jig Data Analysis

Force data and kinematic data were filtered with a second order Butterworth filter with a cutoff frequency one fourth the sampling frequency. Joint angles and angular velocities were calculated between segments. Force data was trimmed to only include data when angular velocity at both joints was below 0.001 rad/s. Moments at each joint as a function of ankle and Tmp angle were computed via static force balance (see Appendix) for each jig configuration and fit to a three dimensional surface (Fig. 3, MATLAB 2017a). The moment surface for the contribution of the exo-tendon to moments at each joint was determined by subtracting the passive moments of the limb without the exo-tendon those with the exo-tendon. This was repeated for each combination of slack lengths and springs.

D. Determination of natural joint moments during walking

Inverse dynamic computations of net joint moments were computed from kinematic and kinetic data collected from an un-augmented bird running down a 5 m track over four force plates space 6 cm apart (AMTI HE6X6 1000 Hz). Markers were placed along centerline of the pelvis (two), at the hip, ankle, Tmp and toe (Fig 2A). Joint moments at Tmp, ankle and knee and hip (as defined in 2A) were calculated via standard 2D planar inverse dynamics[14]Kinematic data collection with exo-tendon

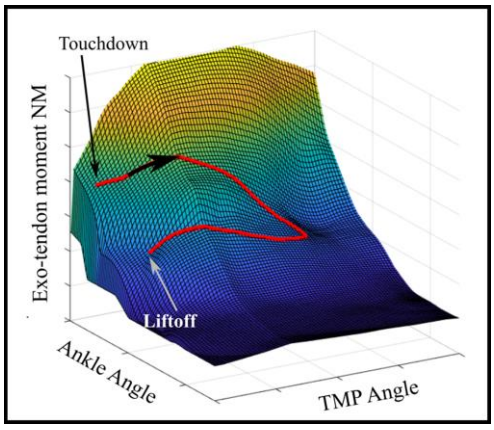

Figure 3 Example moment-angle surface plot with representative stance phase kinematics projected on it in in red.

The bird used to asses locomotor function walked on a treadmill at 1 m/s without exo-tendon and with one stiff and one compliant spring at a consistent slack length while collecting motion capture data as described above but with an 8-camera set-up (4 conditions). Distinctive kinematics events were identified that correlated with toe-off and toe-strike were used to break data into individual strides. Strides were limited to include only those with durations +1 SD of the mean. The resulting kinematics from 24+-17 representative strides per trial were normalized to 101 points per stride and averaged to generate a mean and standard deviation of Tmp, ankle and knee angle as a percentage of time normalized stride duration for each exoskeleton setting (as described above). Data was likewise manipulated to generate time normalized stance kinematics. Joint moments for each condition were interpolated from angle data and the matching moment-angle array established from the jig experiment (Fig 3). Additionally, to evaluate the influence of any change in joint kinematics in response to the exo-tendon, we likewise interpolated for each spring setting the moments that would have been generated if the animal joint kinematics during a stride did not change from kinematics of the bird without the exo-tendon.

E. Statistics

The influence of exo-tendon spring stiffness of joint kinematics was analyzed with two ANOVAs that evaluated the maximum ankle angle and minimum Tmp angle during a stance between kinematics generated while wearing exo-tenon with different stiffness springs.

III. Results

Birds wearing the exo-tendon were able to walk and run on a treadmill with minimal gait disturbance while providing small but influential assistive torques (2.7% of maximum ankle moment, maximum of 2.1% of natural Tmp moment). In response, guinea fowl systematically adjusted joint kinematics with spring stiffness, increasing flexion at the ankle (tending to stretch the exo-tendon, p value < 2e-16) and increasing

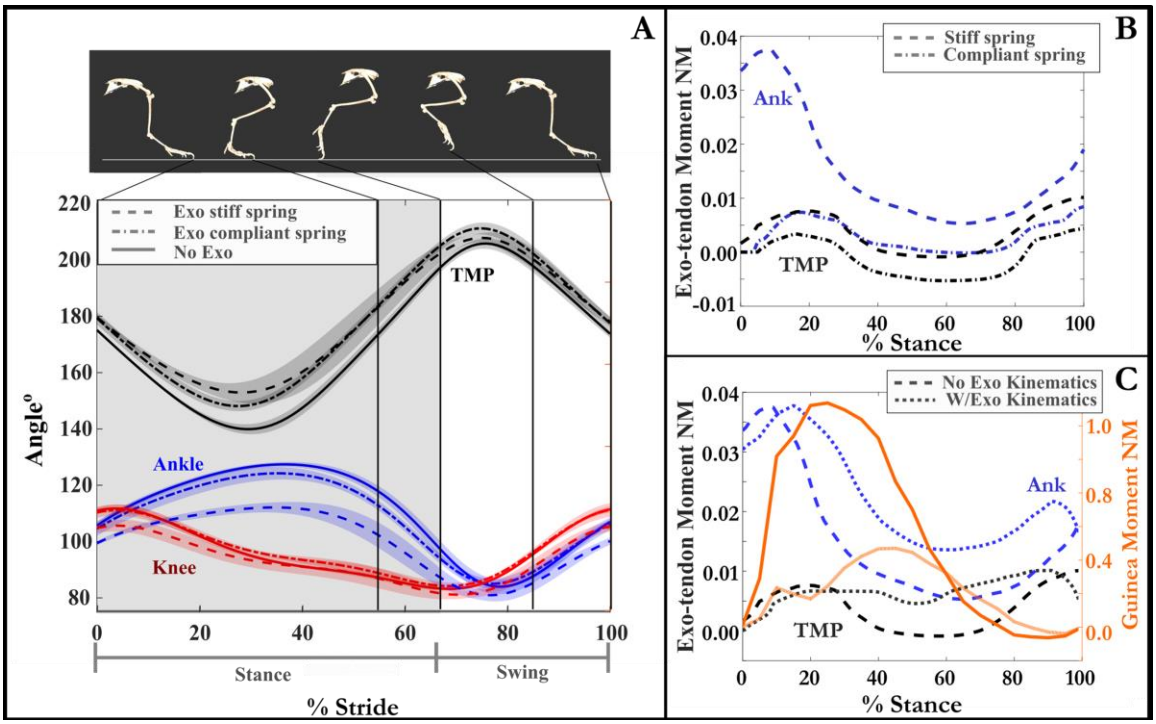

Figure 4 A) A comparison of joint kinematics across a stride with variation in exo-tendon stiffness. With increasing stiffness, TMP angle becomes more flexed while ankle extend. Lines depict means and shaded regions one sd around the mean. B) Changes in exo-tendon moment with spring stiffness during stance at the ankle (blue) and TMP (black) predicted from kinematics collected without the exo-tendon. C) Influence of changing joint kinematics on exo-tendon moment contribution for the stiff spring. Dotted lines depict exo-contribution to joint moments as a result of altered kinematics. Dashed lines represent moments that would have resulted if limb kinematics matched those observed when birds were not wearing the exo-tendon. Natural movement occurring during the stance phase for the ankle (dark orange) and TMP joints (light orange) for a bird without an exo-tendon are included for comparison. Joint kinematics alter the timing of moment contribution more than the magnitude.

extension at the Tmp joint (tending to shorten the exo-tendon, p-value: 9.2e-10). In the absence of this change in kinematics, changes in spring stiffness would have resulted in joint moments that varied four fold at the ankle and two fold at the Tmp joint. The variation in kinematics with spring stiffness did not offload the moment generated by the exo-tendon. Instead varying kinematics altered the timing of maximum exo-tendon moment contribution (Fig 4C).

IV. Discussion

To provide an *in-vivo* platform to explore multi-scale physiological adaptations to assistive wearable robotics we developed a passive-elastic lower-limb exo-tendon for a locomoting animal model, the helmeted guinea fowl. The primary design challenge was to build a device that the birds would tolerate and could provide adjustable assistive torques at the ankle and Tmp joints. This required that the device be small, lightweight and unobtrusive, yet also provide the structure necessary to withstand exo-tendon reaction forces. Early design iterations convinced us to prioritize comfort and minimize mass since designs that did otherwise limited the birds' locomotor capabilities and induced large added mass effects[19]. We found that leather provided the appropriate balance of tensile strength and compliance for the exosuit structure. While leathers with different properties were selected according to the needs of different areas of the device, further reinforcement was still necessary at exo-tendon attachment points to counter deformation.

Minimizing intrusiveness and prioritizing freedom of movement also drove our decision to quantify torque generated by the device using a benchtop calibration rather than instrumenting it with on-board sensors. This approach was preferred both to eliminate the experimental difficulties of the associated wires that on-board sensors would require and to improve accuracy. Measuring exo-tendon torque via its tension (e.g., by using an in series force or strain gauge) would have also required an accurate measurement of the exo-tendon moment arm about both ankle and Tmp at all times. An accurate moment arm measurement would have needed to be determined using an *in situ* 'tendon travel' method, requiring high precision measurements to relate exo-tendon length change to changes in both ankle and Tmp joint angles, a process more complicated and time consuming than our benchtop approach.

The necessity to minimize discomfort and mass of the device resulted in reliance on the morphology of the animal to provide rigidity, rather than an external structure. This came with several tradeoffs. While many human soft exo-suits[7] rely on straps that hook around some horizontal portion of the skeleton to stop the exo-tendon from slipping down the limb, the upper limb of the guinea fowl is cone-like, offering no other feasible anchor points on the leg. Furthermore, birds would not tolerate straps across their backs without disrupting balance. Thus, we anchored the exo-tendon spring on the base of the tibiotarsi above the ankle, a natural location for a proximal attachment point not predisposed to slip from shear

forces. In order to distribute these forces more evenly, the tibial cuff above the ankle was extended proximally and lined with a soft polymer to improved adhesion by maximizing surface area between the device and the skin of the animal[20]. Again, we piggybacked on the integrity of the animal's skeleton to provide structure. This approach also required compressive forces evenly distributed along the tibial cuff, a requirement satisfied by lacing the cuff onto the bird.

While utilizing a soft-exo approach allowed us to build the first successful exoskeleton for a walking animal model, it also reduced the assistive torques we were able to provide. The leather structure deformed before the stiffest springs could strain, minimizing the efficiency of power transmission, as has been observed in other soft exosuit designs[21]. Further, relying on the structure of the bird limited our ability to vary or increase the moment arm about either joint axis, resulting in very small changes in spring length with joint rotation. These combined effects resulted in exo-tendon torques lower than we had intended. In human studies, the greatest energetic benefits from an elastic ankle exoskeleton are observed when the exoskeleton supports ~20% of the naturally occurring joint moment during a stride. We were only able to generate ~1/10 that magnitude in birds.

Further iterations of the exo-tendon design are addressing many of these and other limitations. The reinforcement at the exo-tendon proximal attachment point has been expanded to fully encircle the cuff, allowing laces to distribute spring forces further thoughout. In combination with additional padding along the base of the tibiotarsi, increasing treadmill speed from a brisk walk (1 m/s) to a run (1.5 m/s) should increase the magnitudes of the torques provided by the device that can also be tolerated by the animals. Further, as of yet we have not fully integrated a method to systematically vary slack length to adjust the timing of the exo-tendon spring engagement. We have modified the exo-tendon spring to allow attachment of a small gauge stainless steel chain that can be repeatable adjusted in 5 mm increments. This will enable further work to explore the effect of changing both slack length and spring stiffness on the magnitude and timing of exo-tendon torque support..

Despite what may appear to be limited performance, we still saw systematic changes in joint kinematics with increasing exo-tendon spring stiffness. This suggest that even small assistive torques can consistently change bird behavior. Even more intriguing, the changes in kinematics seem to result in variation of the timing of the exo-tendon's moment contribution rather than altering its magnitude. This is consistent with evidence from human assistive studies as well as isolated muscle experiments that reveal importance of the timing of assistive torques to enhance muscle-tendon dynamics. With a sample size of one, we are far from being able to decode the high level objectives the motor control system uses to adapt to changes in joint mechanics from n exoskeleton, but this preliminary data suggests that our exo-tendon may be sufficiently robust to serve as a platform to assess the direct impact of wearable robots on underlying muscles, tendons and bones.

While many human studies have begun to model[23], [23]–[26] or image[12] physiological adaptations to wearable robotics, our inability to predict the human response to manipulations of elastic systems[4], [27] suggests that our models do not well represent the priorities of the neuromuscular system and highlights gaps between what we can measure on humans and the accuracy of the data necessary to adequately address many questions [2]. Studying how a guinea fowl adapts to a wearable assistive robotic device has several advantages over the present approaches. Guinea fowl are very amenable to in-vivo studies and have long been a model species for 'under the skin' studies of locomotion, from work linking muscle energy use and locomotor mechanics [14], [17], [18], [28] to questions of motor control and stability[16], [29]–[31]. Thus, an adjustable exo-tendon on a guinea fowl would provide a means to directly measure changes in neuromechanics that can at present only be inferred. In addition to *in vivo* work, an *in silico* approach to probe musculoskeletal function can also prove fruitful and has recently expanded to including comparative avian models [32] A guinea fowl musculoskeletal model [33], when paired with in-vivo data could be used to generate informed hypotheses about neural adaptation to exoskeleton augmentation that could then be tested against experimentally collected muscle level data. This could help bridge the gap between modeling predictions about how individual muscle-tendon units should adapt and how they do adapt. Further, an animal model for wearable robotics allows exploration of the physiological or behavioral changes that come with long term exoskeletal use that would not be feasible on humans but are important to understand in order for this field to progress.

The implementation of a soft exo-suit in an avian model system also provides biological inspiration for novel human passive-elastic lower limb orthoses. Unlike humans, digitigrade (toe-running) species such as birds utilize joints distal to the ankle to power legged locomotion[13]. This feature is thought to provide an energetic advantage over human gait [13], [34]. The bird's digitigrade gait guided our design of the two-joint exo-tendon that facilitated simultaneous assistive torque at the ankle and Tmp as well as a natural 'clutch' mechanism to offload the exo-tendon during swing. Implementation of assistive multi-joint elastic exo-tendons to optimize human locomotor energetics has been examined previously using a computational modeling approach[35]. More recently, we have built a two-joint (ankle and metatarso-phalangeal) passive-elastic assistive exo-tendon system for human locomotion [36]. This design emulates the multi-joint muscle-tendon function observed in digitigrade species and is based on parallel design features to those of the current avian exo-tendon. Preliminary tests have found that humans using this two-joint exo-tendon adopt a digitigrade posture and indicate they do so with a reduced energy cost compared to walking without the assistive spring. Complementary studies using our animal exo-tendon framework will provide further guidance for biologically-inspired wearable robotic assistance in humans.

An animal model for wearable robotics opens new paths of research, allowing us to answer questions before inaccessible: What sensorimotor feedback systems modulate neuro-mechanical adaptations to robotic augmentation? What type of long-term augmentation results in neuromechanical and musculoskeletal changes that maximize running efficiency, jumping ability or potential for recovery from neuromuscular injury? How do changes in locomotor performance alter

behavior? How do assistive interventions during growth alter the adult locomotor system? RoboBird is the first in a new wave of tools that will transform the role of robotics in the study of locomotion from simplified models into scientific instruments that allow direct experimental manipulation of biological systems.

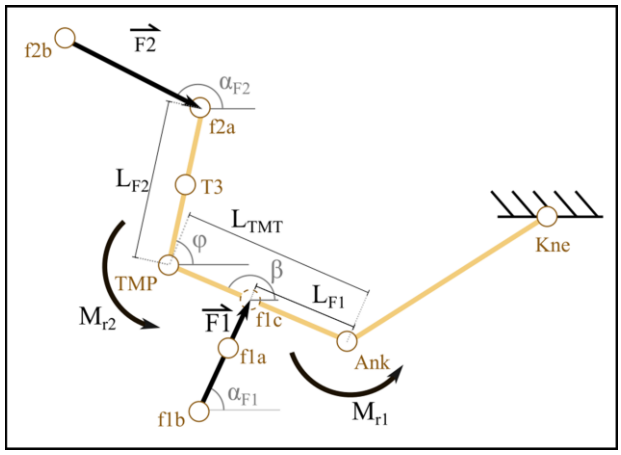

Figure 5 Free body diagram of the benchtop jig

APPENDIX

Jig Moment Calculations

The angle of the line of action of the distal force sensor, F2, from horizontal is given by

$$\alpha_{f2} = atan\left(\frac{f2b_y - f2a_y}{f2b_x - f2a_x}\right). \quad (1)$$

Likewise, the angle of the phalangeal jig segment from horizontal is given by

$$\varphi = \text{atan}\left(\frac{f2a_y - TMP_y}{f2a_x - TMP_x}\right). \quad (2)$$

Thus, for a given force measured at F_2, reaction moment acting at the TMP joint can be given by

$$M_{r2} = -F_2\cos(\alpha_{f2}) * L_{2f}\sin(\varphi) - F_2\sin(\alpha_{f2}) * L_{2f}\cos(\varphi), \quad (3)$$

where L_{F2} is the distance from f2a to TMP (Fig 2B&5). Likewise, the angle of the line of action of the proximal force sensor, f1, from horizontal is given by

$$\alpha_{f1} = \text{atan}\left(\frac{f1b_y - f1a_y}{f1b_x - f1a_x}\right), \quad (4)$$

and the angle of the proximal jig segment is given by

$$\beta = \text{atan}\left(\frac{TMP_y - Ank_y}{TMP_x - Ank_x}\right). \quad (5)$$

The x and y force components of the proximal force sensor can be given by

$$F1_x = F1\sin(\alpha_{f1}), F1_y = F1\cos(\alpha_{f1}). \quad (6)$$

The x and y components of the distance from the proximal force sensor to the ankle joint are

$$L_{TMTx} = L_{TMT}\sin(\beta), L_{TMTy} = L_{TMT}\cos(\beta). \quad (7)$$

And, likewise the x and y components of the moment arm of the proximal force sensor on the proximal jig segment are

$$L_{F1x} = L_{F1}\sin(\beta), L_{F1y} = L_{F1}\cos(\beta). \quad (8)$$

We can write the joint reaction moment acting at the ankle as

$$M_{r1} = -F1_yL_{F1x} - F1_xL_{F1y} + F1_x(L_{TMTy} - L_{F1y}) + F1_y(L_{TMTx} - L_{F1x}). \quad (9)$$

REFERENCES

[1] S. H. Collins, M. B. Wiggin, and G. S. Sawicki, "Reducing the energy cost of human walking using an unpowered exoskeleton," *Nature*, vol. 522, no. 7555, pp. 212–215, 2015.

[2] A. J. Young and D. P. Ferris, "State-of-the-art and Future Directions for Lower Limb Robotic Exoskeletons," vol. 4320, no. c, pp. 171–182, 2016.

[3] S. Viteckova, P. Kutilek, and M. Jirina, "Wearable lower limb robotics: A review," *Biocybern. Biomed. Eng.*, vol. 33, no. 2, pp. 96–105, 2013.

[4] J. Zhang *et al.*, "Human-in-the-loop optimization of exoskeleton assistance during walking," *Science (80-.).*, vol. 1284, no. June, pp. 1280–1284, 2017.

[5] C. Fisahn *et al.*, "The Effectiveness and Safety of Exoskeletons as Assistive and Rehabilitation Devices in the Treatment of Neurologic Gait Disorders in Patients with Spinal Cord Injury : A Systematic Review," *Global*, pp. 822–841, 2016.

[6] S. Maggioni *et al.*, "Robot-aided assessment of lower extremity functions: a review," *J. Neuroeng. Rehabil.*, vol. 13, no. 1, p. 72, 2016.

[7] B. T. Quinlivan *et al.*, "Assistance magnitude versus metabolic cost reductions for a tethered multiarticular soft exosuit," *Sci. Robot.*, vol. 2, no. 2, 2017.

[8] A. A. Biewener, "Muscle-tendon stresses and elastic energy storage during locomotion in the horse," *Comp. Biochem. Physiol. - B Biochem. Mol. Biol.*, vol. 120, no. 1, pp. 73–87, 1998.

[9] T. J. Roberts, "The integrated function of muscles and tendons during locomotion," *Comp. Biochem. Physiol. - A Mol. Integr. Physiol.*, vol. 133, no. 4, pp. 1087–1099, 2002.

[10] A. a Biewener and R. Baudinette, "In vivo muscle force and elastic energy storage during steady-speed hopping of tammar wallabies (Macropus eugenii)," *J. Exp. Biol.*, vol. 198, pp. 1829–41, 1995.

[11] J. M. Florez *et al.*, "Rehabilitative Soft Exoskeleton for Rodents," *IEEE Trans. Neural Syst. Rehabil. Eng.*, vol. 25, no. 2, pp. 107–118, 2017.

[12] D. J. Farris, B. D. Robertson, and G. S. Sawicki, "Elastic ankle exoskeletons reduce soleus muscle force but not work in human hopping," *J. Appl. Physiol.*, vol. 115, no. 5, pp. 579–585, 2013.

[13] J. Rubenson, D. G. Lloyd, D. B. Heliams, T. F. Besier, and P. a Fournier, "Adaptations for economical bipedal running: the effect of limb structure on three-dimensional joint mechanics.," *J. R. Soc. Interface*, vol. 8, no. 58, pp. 740–755, 2011.

[14] J. Rubenson and R. L. Marsh, "Mechanical efficiency of limb swing during walking and running in guinea fowl (Numida meleagris)," *J. Appl. Physiol.*, vol. 106, no. 1985, pp. 1618–1630, 2009.

[15] M. A. Daley and A. A. Biewener, "Muscle force – length dynamics during level versus incline locomotion : a comparison of in vivo performance of two guinea fowl ankle extensors," *J. Exp. Biol.*, vol. 206, pp. 2941–2958, 2003.

[16] M. A. Daley and A. A. Biewener, "Leg muscles that mediate stability : mechanics and control of two distal extensor muscles during obstacle negotiation in the guinea fowl," *Philos. Trans. R. Soc. B Biol. Sci.*, vol. 366, pp. 1580–1591, 2011.

[17] D. J. Ellerby and R. L. Marsh, "The energetic costs of trunk and distal-limb loading during walking and running in guinea fowl Numida meleagris II . Muscle energy use as indicated by blood flow," pp. 2064–2075, 2006.

[18] J. Rubenson, H. T. Henry, P. M. Dimoulas, and R. L. Marsh, "The cost of running uphill : linking organismal and muscle energy use

in guinea fowl (Numida meleagris)," pp. 2395–2408, 2006.
[19] R. L. Marsh, D. J. Ellerby, H. T. Henry, and J. Rubenson, "The energetic costs of trunk and distal-limb loading during walking and running in guinea fowl Numida meleagris I . Organismal metabolism and biomechanics," pp. 2050–2063, 2006.
[20] D. R. King and A. J. Crosby, "Optimizing Adhesive Design by Understanding Compliance," *ACS Appl. Mater. Interfaces*, vol. 7, no. 50, pp. 27771–27781, 2015.
[21] M. B. Yandell, B. T. Quinlivan, D. Popov, C. Walsh, and K. E. Zelik, "Physical interface dynamics alter how robotic exosuits augment human movement: implications for optimizing wearable assistive devices," *J. Neuroeng. Rehabil.*, vol. 14, no. 1, pp. 1–11, 2017.
[22] G. S. Sawicki, B. D. Robertson, E. Azizi, and T. J. Roberts, "Timing matters: tuning the mechanics of a muscle-tendon unit by adjusting stimulation phase during cyclic contractions," *J. Exp. Biol.*, vol. 218, no. 19, pp. 3150–3159, 2015.
[23] D. J. Farris, J. L. Hicks, S. L. Delp, and G. S. Sawicki, "Musculoskeletal modelling deconstructs the paradoxical effects of elastic ankle exoskeletons on plantar-flexor mechanics and energetics during hopping," *J. Exp. Biol.*, vol. 217, no. 22, pp. 4018–4028, 2014.
[24] R. W. Jackson, C. L. Dembia, S. L. Delp, and S. H. Collins, "Muscle–tendon mechanics explain unexpected effects of exoskeleton assistance on metabolic rate during walking," *J. Exp. Biol.*, vol. 220, no. 11, pp. 2082–2095, 2017.
[25] B. D. Robertson, D. J. Farris, and G. S. Sawicki, "More is not always better: modeling the effects of elastic exoskeleton compliance on underlying ankle muscle-tendon dynamics," *Bioinspir. Biomim.*, vol. 9, no. 4, 2014.
[26] G. S. Sawicki and N. S. Khan, "A simple model to estimate plantarflexor muscle-tendon mechanics and energetics during walking with elastic ankle exoskeletons," *IEEE Trans. Biomed. Eng.*, vol. 63, no. 5, pp. 914–923, 2016.
[27] D. P. Ferris, G. S. Sawicki, and M. A. Daley, "A physiologist's perspective on robotic exoskeletons for human locomotion," *Int J HR*, vol. 4, no. 3, 2007.
[28] R. L. Marsh, D. J. Ellerby, J. A. Carr, H. T. Henry, and C. I. Buchanan, "Partitioning the Energetics of Walking and Running : Swinging the Limbs Is Expensive," vol. 303, no. January, pp. 80–83, 2004.
[29] M. A. Daley, J. R. Usherwood, G. Felix, and A. A. Biewener, "Running over rough terrain : guinea fowl maintain dynamic stability despite a large unexpected change in substrate height," *J. Exp. Biol.*, vol. 209, pp. 171–187, 2006.
[30] A. V. Birn-Jeffery and M. A. Daley, "Birds achieve high robustness in uneven terrain through active control of landing conditions," *J. Exp. Biol.*, vol. 215, no. 12, pp. 2117–2127, 2012.
[31] J. C. Gordon, J. W. Rankin, and M. A. Daley, "How do treadmill speed and terrain visibility influence neuromuscular control of guinea fowl locomotion?," *J. Exp. Biol.*, vol. 218, pp. 3010–3022, 2015.
[32] J. W. Rankin, J. Rubenson, and J. R. Hutchinson, "Inferring muscle functional roles of the ostrich pelvic limb during walking and running using computer optimization," *J. R. Soc. Interface*, vol. 13, no. 118, p. 20160035, 2016.
[33] J. Rubenson, H. Sanghvi, M. J. Cromie, K. Easton, R. L. Marsh, and S. L. Delp, "Influence of tendon compliance and activation level on fibre operating lengths of skeletal muscle," in *Anual Meeting of the Society-for-Integrative-andComparative-Biology*, 2013, p. San Fancisco, CA.
[34] A. M. Wilson, A. J. Van den Bogert, and M. P. McGuigan, "Optimization of the muscle-tendon unit for economical locomotion," in *Skeletal muscle mechanics: from mechanism to function*, W. Herzog, Ed. Hoboken, NJ: John Wiley & Sons, 2000, pp. 517–47.
[35] A. J. van den Bogert, "Exotendons for assistance of human locomotion," *Biomed. Eng. Online*, vol. 2, pp. 1–8, 2003.
[36] B. A. Green, G. S. Sawicki, and J. Rubenson, "Energy cost of walking in a passive-elastic ankle-metatarsophalangeal exoskeleton," in *41st Annual meeting of the American Socieity of Biomechanics*, 2017.